

Heavy element contributions of rotating massive stars to Interstellar Medium *

Ruiqing Wu¹, Chunhua Zhu¹, Guoliang Lü¹, Zhaojun Wang¹, Helei Liu¹

School of Physical Science and Technology, Xinjiang University, Urumqi 830046, China;
ruiqingwu163@163.com, chunhuazhu@sina.cn

Received 2020 December 9; accepted 2021 January 12

Abstract Employing the the stellar evolution code (Modules for Experiments in Stellar Astrophysics), we calculate yields of heavy elements from massive stars via stellar wind and core–collapse supernovae (CCSN) ejecta to interstellar medium (ISM). In our models, the initial masses (M_{ini}) of massive stars are taken from 13 to $80 M_{\odot}$, their initial rotational velocities (V) are 0, 300 and 500 km s^{-1} , and their metallicities are $[Fe/H] = -3, -2, -1, \text{ and } 0$. The yields of heavy elements coming from stellar winds are mainly affected by the stellar rotation which changes the chemical abundances of stellar surfaces via chemically homogeneous evolution, and enhances mass-loss rate. We estimate that the stellar wind can produce heavy element yields of about 10^{-2} (for low metallicity models) to several M_{\odot} (for low metallicity and rapid rotation models) mass. The yields of heavy element produced by CCSN ejecta also depend on the remnant mass of massive mass which is mainly determined by the mass of CO-core. Our models calculate that the yields of heavy elements produced by CCSN ejecta can get up to several M_{\odot} . Compared with stellar wind, CCSN ejecta has a greater contribution to the heavy elements in ISM. We also compare the ^{56}Ni yields by calculated in this work with observational estimate. Our models only explain the ^{56}Ni masses produced by faint SNe or normal SNe with progenitor mass lower than about $25 M_{\odot}$, and greatly underestimate the ^{56}Ni masses produced by stars with masses higher than about $30 M_{\odot}$.

Key words: Stars: massive—rotation—ISM: abundances

1 INTRODUCTION

Interstellar medium (ISM) is defined as follows: atomic, gas ions, dust grains, cosmic rays, and also includes many molecules. Heavy elements are fundamental components to ISM and play a critical role in the stellar evolution of astrophysics and the chemical evolution in the ISM. It is well known that massive stars with a initial mass larger than $\sim 8M_{\odot}$ play the most important role for producing the heavy elements in ISM (e. g., [Dunne et al. 2003](#); [Ablimit & Maeda 2018](#); [Du 2020](#)). These massive stars contribute to heavy elements via stellar wind and the ejecta of core–collapse supernovae (CCSN). Although the heavy elements may originate from other sources including the stellar wind of asymptotic giant branch stars, ejecta of classical novae, binary merger et al, their contribution is very low ([Groenewegen & de Jong 1993](#); [Marigo 2007](#); [Hix 2001](#); [Lü et al. 2013](#); [Zhu et al. 2013](#); [José et al. 2006](#); [Li et al. 2016](#); [Rukeya et al. 2017](#); [Zhu et al. 2019](#); [Duolikun et al. 2019](#); [Shi et al. 2020](#); [Guo et al. 2020](#)).

* Supported by the National Natural Science Foundation of China.

The yields of heavy elements from massive stars have been investigated by many literatures (e. g., Woosley & Weaver 1995; Chieffi & Limongi 2004; Nomoto et al. 2006; Heger & Woosley 2010; Nomoto et al. 2013). However, these works do not consider mass loss which is very important for the massive star evolution (A recent review can be seen in Smith 2014). Usually, the mass loss was thought to be caused by stellar wind driven by drastic radiation (Castor et al. 1975; Puls et al. 2008). Simultaneously, it is also affected by metallicity and rotation (Vink 2000; Vink et al. 2001; Meynet 2000; Maeder & Meynet 2012). Because the efficiency of radiation pressure removing the stellar envelope depends on metallicity, it has an effect on the mass-loss rates (\dot{M}) of massive stars by $\dot{M} \propto Z^m$, where the index range of m is from 0.5 to 0.94 (Vink 2000; Vink et al. 2001; Mokiem et al. 2007). Rotation can enhance the mass-loss rate (Langer et al. 1998; Heger 1998). More importantly, rapidly rotation can result in quasi chemically homogeneous evolution (CHE) induced by various instability, such as dynamical shear instability, the Solberg-Hilòland instability, the secular shear instability, the Eddington-Sweet circulation, and the Goldreich Schubert-Fricke instability (e. g., Pinsonneault et al. 1989; Heger & Langer 2000). CHE can carry the heavy elements produced by nuclear burning in the core to the stellar surface, thus these heavy elements enter ISM via stellar wind (e. g., Brott et al. 2011; Song et al. 2016; Cui et al. 2018). The role of heavy elements mixing is critical, it will affect the opacity of the envelope and increase the luminosity and effective temperature of the star (Glebbeek et al. 2009).

The standard non-rotating single-star model is strongly opposed as a possible progenitor of the Supernovae (SNe) (Fremming et al. 2014; Bersten & Nomoto 2014a). But Prantzos et al. (2018) recently gave the heavy element yields of rotating massive stars. They considered effects of three initial rotational velocities, namely, 0, 150 and 300 km s⁻¹. Initial velocity above ~ 350 km s⁻¹ more likely attain to the critical velocity (Meynet & Maeder 2006). Furthermore, in the VLT-FLAMES Tarantula Survey, Dufton et al. (2013) found that the projected rotational velocities of single early B-type stars can reach approximately 450 km s⁻¹. In binary systems, owing to mass transfer rotation velocity will reach to the Kepler velocity (de Mink et al. 2013).

Meanwhile, rapidly rotation result in a more massive helium core via CHE (Belczynski et al. 2016; Eldridge & Maund 2016; Mandel & De Mink 2016; Marchant et al. 2016; Wang et al. 2018). On account of the helium-core masses have greatly effects on the remnant masses of neutron stars and black holes (e. g., Hurley et al. 2000; Belczynski et al. 2008). At the pre-supernova (pre-SN) stage, a larger helium-core burning produces a bigger CO-core (Meynet & Maeder 2006; Köhler et al. 2015; Marassi et al. 2019). Hence, rotation as well as affects the heavy elements of CCSN ejecta. Very recently, in order to study dust formation in CCSN ejecta, Marassi et al. (2019) considered the effects of rotation, metallicity, and fallback, they computed the heavy element yields of massive stars. However, they did not still considered the yields via stellar wind.

Therefore, it is necessary to study the heavy element yields coming from stellar wind and CCSN ejecta for massive stars. Even the research on the relevant factors of elemental abundance is very urgent. In this paper, we study the effects of metallicity, rotation and fallback on the contribution of heavy elements produced by massive stars. In Section 2, the input physical parameters in models are described. The detailed results are discussed in Section 3. The main conclusions appear in Section 4.

2 MODEL

We use the open-source stellar evolution code Modules Experiments in Stellar Astrophysics (MESA, version 10108, model core-collapsed supernova) to simulate massive star evolutions (Paxton et al. 2011, 2013, 2015). In these simulations, we select 67–isotope network. The mixing-length parameter (α_{mlt}) is taken as 1.5 (Brott et al. 2011; Moravveji 2016; Ma et al. 2020; Shi et al. 2020). In addition, the Ledoux criterion connects with boundaries of convection, semi-convection (α_{sc}) is selected as 0.02. Most of all, MESA has the Ledoux criterion $\nabla = \nabla_{\text{rad}}$ in the overshoot area, which is different with deep overshoot method (Maeder 1975; Viallet et al. 2015). Overshooting between convective core and radiative of interior diffusion parameter is expressed by ($f_{\text{ov}} = 0.05$). Another effective parameter ($f_{\text{o}} = 0.02$) is from the surface down to overshoot layer, (Paxton et al. 2011; Moravveji 2016; Higgins & Vink 2019), they are considered at all stages of evolution, they also can affect the total mass of stellar

loss. Thermohaline mixing parameter (α_{th}) is equal to 2.0 (Kippenhahn et al. 1980; Paxton et al. 2013). In this work, we use the formulae of Vink et al. (2001) to calculate the mass-loss rates. In addition, rotation can enhance mass-loss rate by

$$\dot{M}(\Omega) = \left(\frac{1}{1 - \Omega/\Omega_{\text{crit}}} \right)^\gamma \dot{M}(0), \quad (1)$$

where $\dot{M}(0)$ is the mass-loss rate without rotation, Ω and Ω_{crit} represent the angular velocity and critical Keplerian angular velocity, respectively, and parameter γ equals 0.43 (Langer et al. 1998). $\dot{M}(0)$ is calculated by the formulae in Vink et al. (2001). But when the angular velocity reaches the critical angular velocity, there will be a singularity. We limit the mass loss rate so that the mass loss time scale is longer than the thermal time scale of the star, see (1)-(3) equations in Yoon et al. (2012).

In order to discuss the effects of metallicity, the 4 initial metallicities are taken in different models as follows: $[Fe/H] = 0$, $[Fe/H] = -1$, $[Fe/H] = -2$ and $[Fe/H] = -3$. Here, $[Fe/H] = \log[(Fe/H)/(Fe/H)_\odot]$ where $[Fe/H]_\odot = 0.02$ is the solar metallicity (Thielemann et al. 2010; Chiaki et al. 2015).

Considering that rotational velocity of massive stars may get up to the critical velocity (de Mink et al. 2013) at the stellar surface, we take the initial rotational velocities in different simulations as 0, 300 and 500 km s^{-1} , respectively. Rotation triggers some instabilities, then lead to angular momentum transport and chemical mixing (e. g., Meynet 2012). Based on the research of Pinsonneault et al. (1989), Heger & Langer (2000) and Yoon & Langer (2006), MESA uses the ratio of the turbulent viscosity to the diffusion coefficient (f_c) and the ratio of sensitivity to chemical gradients (f_μ) to calculate angular momentum transport and chemical mixing induced by rotation. Zhu et al. (2017) and Cui et al. (2018) employed MESA to investigate rotating massive stars. Following them, we choose $f_c = 0.0228$ and $f_\mu = 0.1$, respectively.

MESA code can calculate the stellar evolution from pre-main sequence to CCSN. However, it can not give the remnant masses after CCSN. In our work, following Hurley et al. (2000); Belczynski et al. (2008); Wang et al. (2018) the remnant masses of NS or BH are given by CO-core mass. CCSNe model of the MESA via collapsing of an core when the mass of Fe core $> 1.4 M_\odot$, and we do not consider the nuclear reaction in this stage. The explosion mechanism of CCSNe is a complex process which is still has not been well explained. In our model the explosion energy (E) is 1×10^{51} ergs (Nomoto et al. 2007; Paxton et al. 2013; Hirschi et al. 2017; Curtis et al. 2019).

Simultaneously, a supernova explosion occurs when stellar central density gets to $7.9 \times 10^9 \text{ g/cm}^3$ and central temperature is $\sim 6.5 \times 10^9 \text{ K}$.

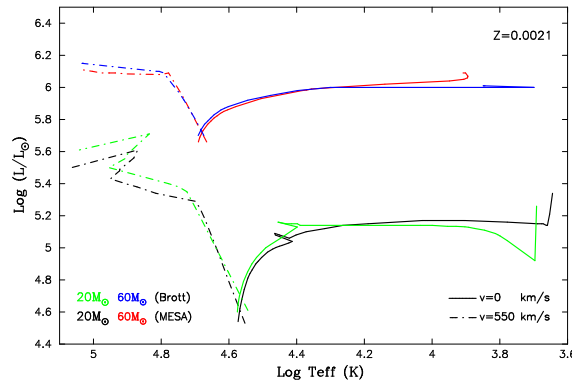


Fig. 1: The evolutions of massive stars with different masses and rotation velocities for $Z = 0.0021$. The solid lines represent a non-rotating star, while the dash-dotted lines represent a star with a rotation velocity of 550 km s^{-1} . Green and blue lines are the evolutionary tracks calculated by Brott et al. (2011), and black and red lines are simulated in our models.

3 RESULTS

Using MESA code, we simulate the evolutions from main sequence (MS) to CCSN for 8 massive stars with masses of 13, 15, 20, 25, 30, 40, 60 and 80 M_{\odot} . In order to discuss the effects of rotation, the initial rotational velocities are taken 0, 300 and 500 km s^{-1} in different simulations, respectively. In order to check our model, we compare the evolutions of several stars with these in [Brott et al. \(2011\)](#) under similar input parameters. Figure 1 shows the evolutionary tracks in two works are similar. All heavy elements originating from star are produced by nucleosynthesis. They are ejected into ISM via stellar wind and CCSN ejecta.

3.1 Heavy elements coming from stellar wind

Before massive stars occur CCSN, their heavy elements enter ISM via stellar winds. These heavy elements locate in stellar envelope. In this work, we estimate the yields of i -th heavy element by

$$M_i = \int_0^{t_{\text{pre}}} \dot{M}(t) X_i(t) dt, \quad (2)$$

where t_{pre} is the time from zero-age MS to pre-CCSN, $\dot{M}(t)$ and $X_i(t)$ are the mass-loss rate and the mass fraction of i -th heavy element on the surface of massive star, respectively. Therefore, the heavy elements coming from stellar wind mainly depend on the mass-loss rates and the chemical abundances on the stellar surface.

In our model, the mass-loss rates are affected by metallicity and rotational velocity. Figure 2 shows the evolutions of mass-loss rates for different initial mass stars with different metallicities and rotational velocities.

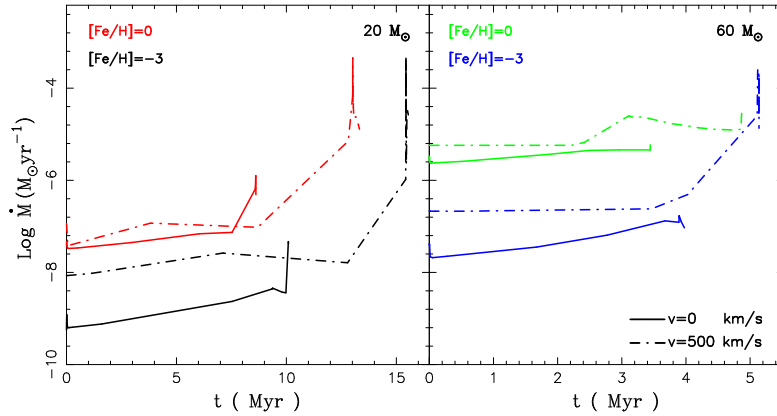


Fig. 2: The evolutions of mass-loss rates for models with different masses (20 and 60 M_{\odot}), metallicities ($[Fe/H] = 0, -3$) and rotational velocities (0 and 500 km s^{-1}).

Compared the two metallicities models, a high metallicity can result in a high mass-loss rate because $\dot{M} \propto Z^m$, where parameter m ranges from 0.64 to 0.85 ([Vink et al. 2001](#)). Simultaneously, the mass-loss rates depends on the rotational velocities by Eq. 1 mainly for MS stage, we also consider the red supergiant (RSG) or Wolf-Rayet (WR) stage ([Nugis & Lamers 2000](#)). Therefore, the higher the initial rotational velocity is, the higher the mass-loss rates is. The mass-loss rate can be enhanced about 1-4 magnitude when the initial rotational velocity increases from 0 to 500 km s^{-1} . The chemical abundances on stellar surfaces are determined by CHE. During MS late phase, the star begins to rapidly expand, the rotational velocity sharply decrease. Therefore, CHE mainly works in MS phase. The heavy elements affected by nucleosynthesis during MS phase are ^{12}C , ^{14}N and ^{16}O (key elements of the evolution of massive stars).

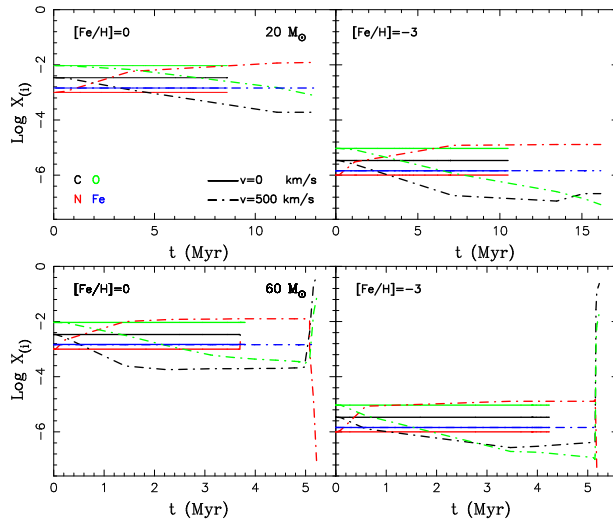


Fig. 3: The evolutions of heavy-element abundances [^{12}C (black), ^{14}N (red), ^{16}O (green), and ^{56}Fe (blue)] on the stellar surfaces for massive stars. The two panels in the top region represent the models with $20 M_{\odot}$, while the two panels in the bottom region is for $60 M_{\odot}$. The solid and dash-dotted lines represent models with $V = 0$ and 500 km s^{-1} , respectively. The different metallicities are given in the left-top region of every panel.

Figure 3 gives the evolutions of heavy-element (^{12}C , ^{14}N and ^{16}O) abundances on the stellar surfaces. Obviously, if there is no CHE in models without rotation, the heavy-element abundances on the stellar surface are constant during its life. However, in rotational models, the abundances of ^{12}C , ^{14}N and ^{16}O elements on the stellar surfaces change. ^{12}C and ^{16}O abundance decreases, while ^{14}N abundances increases. In particular, the lower metallicity is, the stronger CHE is. Therefore, for lower metallicity models, the range of increase and decrease in abundance is more obvious. In addition, for $60 M_{\odot}$ panel, because the H-rich shell are stripped out before the RSG phase, and the star come in a WR stage. As Figure 3 shows, ^{12}C and ^{16}O elements under stellar surface deeply increase while ^{14}N elements decreases. Similar results have been discussed in Maeder & Meynet (2001), Hirschi et al. (2005), Chieffi & Limongi (2013), Groh et al. (2014), and Meyer et al. (2020).

Figure 4 gives the yields of heavy elements (^{12}C , ^{14}N , ^{16}O , and ^{56}Fe) produced via stellar winds. Hirschi et al. (2005b) also calculated the yields of heavy elements produced by stellar winds. In the Table 3 for a model with $M_{\text{ini}} = 20 M_{\odot}$, $[Fe/H] = 0$ and $V = 300 \text{ km s}^{-1}$, Hirschi et al. (2005b) gave the yields of ^{12}C , ^{14}N , ^{16}O elements are 1.73×10^{-2} , 4.30×10^{-2} and $2.75 \times 10^{-2} M_{\odot}$, respectively. Under similar input parameters, the yields in our models are 3.34×10^{-2} , 7.20×10^{-2} , and $4.32 \times 10^{-2} M_{\odot}$, respectively. For a model with $M_{\text{ini}} = 40 M_{\odot}$, they in Hirschi et al. (2005b) are 1.60, 1.73×10^{-1} and $3.34 \times 10^{-1} M_{\odot}$, respectively. They in our work are 1.15, 1.74×10^{-1} and $3.13 \times 10^{-1} M_{\odot}$, respectively. The results in both works are consistent.

In short, the yields of heavy elements coming from stellar winds can get to several M_{\odot} for high rotation and high metallicity, while they may only be $10^{-2} M_{\odot}$ for low rotation and low metallicity.

3.2 Heavy elements coming from SN ejecta

The heavy elements locating in stellar interiors are ejected into ISM via CCSN. They are mainly determined by mass fractions before CCSN occurs. Figure 5 and Figure 6 show the fractions of different elements in the models. For models with a mass of $20 M_{\odot}$, rapid rotation can enhance mass-loss rates. The star with $V = 500 \text{ km s}^{-1}$ have lost whole hydrogen envelope. Simultaneously, it can trigger CHE, produce a larger CO-core. Therefore, compared with the star without rotation, it has more massive core

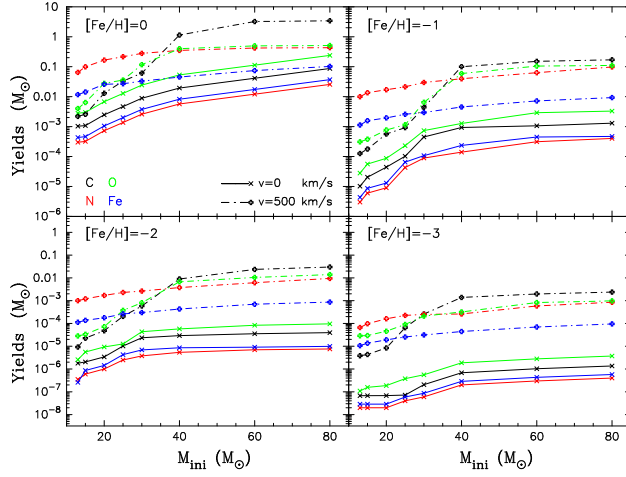


Fig. 4: The yields of the heavy elements, ^{12}C (black), ^{14}N (red), ^{16}O (green), and ^{56}Fe (blue), produced via stellar winds from massive stars with different initial masses, metallicities ($[Fe/H] = 0, -1, -2, -3$), and $V = 0, 500 \text{ km s}^{-1}$. The multiplication and addition symbols represent calculated models with $V = 0$ and 500 km s^{-1} , respectively.

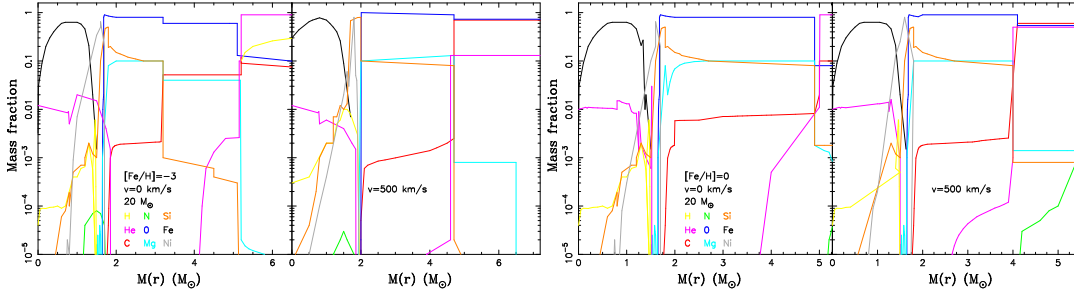


Fig. 5: The mass fractions of chemical elements in stellar interiors $[M(r)]$ at pre-CCSN for models with initial mass of $20 M_{\odot}$. The left two panels (the initial rotational velocities are 0 and 500 km s^{-1} , respectively) represent the models with $[Fe/H] = -3$, and the right two panels for the models with $[Fe/H] = 0$. The abundance of various chemical elements is represented by colorful lines, for example, ^1H (yellow), ^{12}C (red), ^{14}N (green) etc.

before CCSN. The stars with low metallicity can undergoes efficient CHE and have low mass-loss rate. Their CO-core at pre-CCSN are larger than those for the stars with high metallicity. Similar results appear in models with $60 M_{\odot}$ star. These results are consistent with these in [van Marle et al. \(2007\)](#); [Tominaga \(2008\)](#); [Limongi & Chieffi \(2018\)](#). During CCSN, massive stars eject a portion of their masses and leave compact objects (neutron stars or black holes). Generally, the remnant mass (M_{rem}) is calculated by CO-core mass (M_{CO}) (e. g., [Belczynski et al. 2008](#)). In this work, we use the Equations (1) to (4) in [Belczynski et al. \(2008\)](#) to calculate M_{rem} .

Figure 7 (Left) gives M_{CO} and M_{rem} calculated by different models. M_{CO} and M_{rem} are mainly determined by mass-loss rates. The stars with high metallicity and high rotational velocity have high mass-loss rates, their M_{CO} and M_{rem} hardly exceed $10 M_{\odot}$. CHE triggered by rapid rotation can only increase the M_{CO} and M_{rem} of models with initial masses lower than about $30 M_{\odot}$. We compare the CO-core with the work of [Belczynski et al. \(2008\)](#) model with a rotation of 300 km s^{-1} , obviously the size of the CO-core of the two models are consistent.

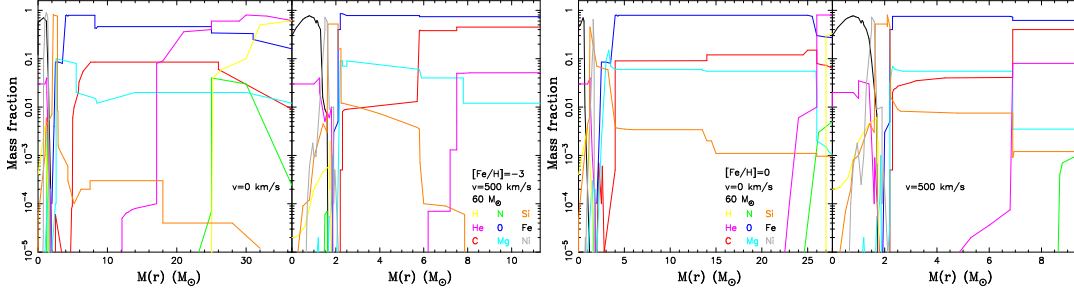


Fig. 6: Similar with Figure 5 but for models with initial mass of $60 M_{\odot}$.

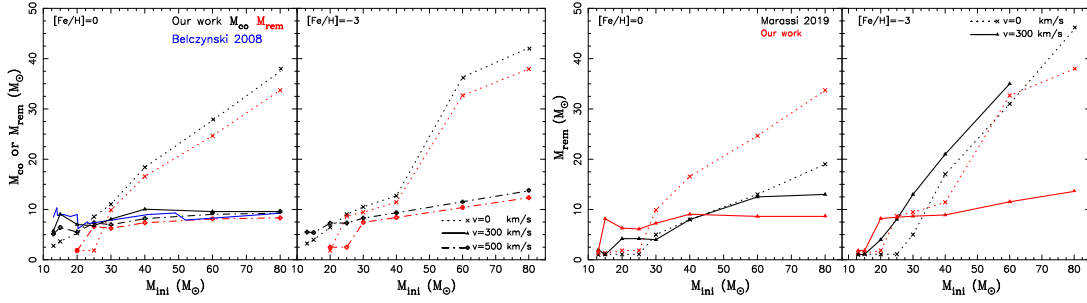


Fig. 7: Left: the CO-core (M_{CO}) and remnant (M_{rem}) masses vs. The initial masses in different models. The black and the red lines represent M_{CO} and M_{rem} , respectively (Our work). The solid blue line represents the CO-core size of the [Belczynski et al. \(2008\)](#) model with a rotation of 300 km s^{-1} . Right: comparison of the remnant masses in our work with those in [Marassi et al. \(2019\)](#). Black and red lines represent [Marassi et al. \(2019\)](#) results and ones in our.

Figure 7 (Right) compares M_{rem} calculated by this work with those in [Marassi et al. \(2019\)](#). Obviously, M_{rem} of stars with initial masses lower than about $30 M_{\odot}$ in our work is higher than that in [Marassi et al. \(2019\)](#), while others in our work are lower. The main reasons are mass-loss rates and the method for calculating remnant mass. For the former, as Figure 2 in [Marassi et al. \(2019\)](#) showed, the hydrogen envelope with a mass of about $3 M_{\odot}$ in the model with $60 M_{\odot}$ initial mass and $[\text{Fe}/\text{H}]=-1$ is left before CCSN. However, under the model with $[\text{Fe}/\text{H}]=-1$, there is no hydrogen envelope for $60 M_{\odot}$ initial mass at pre-CCSN. For the latter, the remnant mass in [Marassi et al. \(2019\)](#) is determined by the initial mass and the metallicity, while this work calculates M_{rem} via M_{CO} . Observation show that the CO nucleus will only appear when the gas density of the star reaches the standard value [Chen et al. \(2006\)](#). The yield of the i -th element produced by CCSN ejecta can be calculated by explosion.

Figure 8 shows the yields of heavy elements produced by CCSN ejecta in this work.

$$M_i = \int_{M_{rem}}^{M_{fin}} [X_i(m) - X_i^0] dm \quad (3)$$

where $X_i(m)$ is the i -th element mass fraction before the SN with Lagrangian coordinate m , X_i^0 is the initial abundance, the X_i^0 of these elements are 0. M_{fin} is the final mass of the star [Ekström et al. \(2008\)](#). However, compared with stellar winds (see Figure 4), CCSN ejecta can produce more heavy elements, especially the elements heavier than ^{16}O element. Compared with [Marassi et al. \(2019\)](#), our work gives lower yields of heavy elements. The main reason is that our models have higher mass-loss rates. Before CCSN occurs, the stars in our models have lost more mass than those in [Marassi et al. \(2019\)](#).

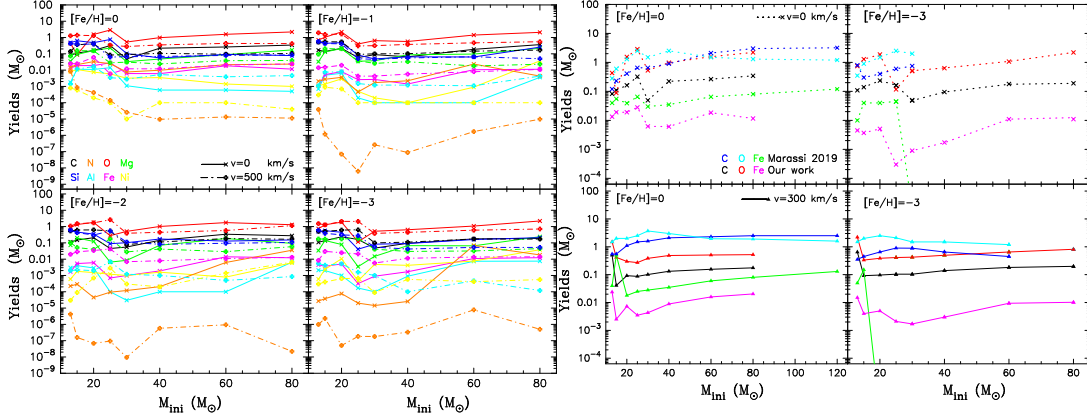


Fig. 8: Yields of heavy elements produced by CCSN ejecta. The left panel represents the results in this work. The right panel gives the comparison of our results with ones in [Marassi et al. \(2019\)](#).

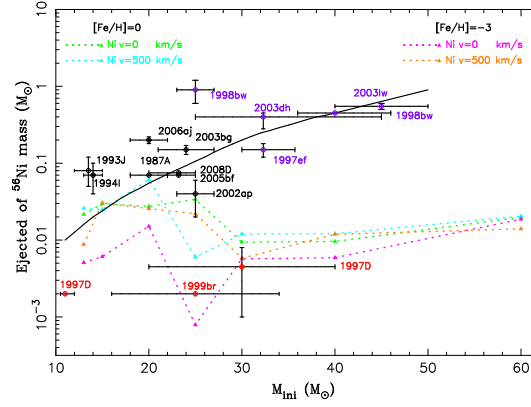


Fig. 9: The ^{56}Ni masses produced by CCSN ejecta and their progenitor masses at MS phase. These data come from [Nomoto et al. \(2013\)](#). The red, black and purple cycles represent faint SNe, normal SNe and hypernovae, respectively. The yields of ^{56}Ni calculated by our models are given by dotted lines ($[Fe/H] = 0$) and dashed lines ($[Fe/H] = -3$). For example, the green and blue colors represent models with $V = 0$ and 500 km s^{-1} , respectively.

Via the comparison of observed light curves and the theoretical models, [Nomoto et al. \(2013\)](#) estimated the ^{56}Ni masses produced by some CCSN ejecta and their progenitor masses, which are showed in Figure 9. Here, ^{56}Ni is caused by the decay of $^{56}\text{Ni} \rightarrow ^{56}\text{Co} \rightarrow ^{56}\text{Fe}$ ([Argast et al. 2002](#); [Hamuy 2003](#)). We calculate the yields of ^{56}Ni in the different initial mass models. Similar with the fixed energy models in [Marassi et al. \(2019\)](#), our results only explain the ^{56}Ni masses produced by faint SNe or normal SNe with progenitor mass lower than $25 M_{\odot}$. Clearly, our understanding for the massive star evolution and CCSN is still poor.

4 CONCLUSIONS

In this work, we calculate the contribution of heavy elements from massive stars via stellar wind and CCSN ejecta to ISM.

In our models, the evolutions of massive stars are affected by rotation, mass-loss rate and metallicity. The rotation via CHE changes the chemical abundances of stellar surfaces, and enhances mass-loss rate.

It can increase ^{14}N abundance by 10 times while decrease ^{12}C and ^{16}O abundances by similar times. It can enhance the mass-loss rates by about 1-4 magnitude when the initial rotational velocity increases from 0 to 500 km s^{-1} . Therefore, the yields of heavy elements coming from stellar winds are mainly affected by the stellar rotation. We estimate that the stellar wind can produce heavy element yields of about 10^{-2} (for low metallicity models) to several M_{\odot} mass (for low metallicity and rapid rotation models), which depends on stellar rotation and metallicity.

The yields of heavy element produced by CCSN ejecta depend on not only rotation, mass-loss rate and metallicity, but also the remnant mass of massive mass. Here, the latter mainly depends on the mass of CO-core which is greatly affected by the above three parameters. Our models calculate that the yields of heavy elements produced by CCSN ejecta can get up to several M_{\odot} mass. Compared with stellar wind, CCSN ejecta have a greater contribution to the heavy elements in ISM.

We also compare the ^{56}Ni yields by calculated in this work with observational estimate. Our models only explain the ^{56}Ni masses produced by faint SNe or normal SNe with progenitor mass lower than about $25 M_{\odot}$, and greatly underestimate the ^{56}Ni masses produced by stars with initial masses higher than about $30 M_{\odot}$. It means that there is still a long way to understand the massive star and CCSN evolution.

Acknowledgements This work received the generous support of the National Natural Science Foundation of China, projects No. 11763007, 11863005, 11803026, and U2031204. We would also like to express our gratitude to the Tianshan Youth Project of Xinjiang No. 2017Q014.

References

- Ablimit, I., & Maeda, K. 2018, *ApJ*, 866, 151 [1](#)
- Argast, D., Samland, M., Thielemann, F. K., & Gerhard, O. E. 2002, *A&A*, 388, 842 [8](#)
- Belczynski, K., Kalogera, V., Rasio, F. A., et al. 2008, *ApJS*, 174, 223 [2](#), [3](#), [6](#), [7](#)
- Belczynski, K., Heger, A., Gladysz, W., et al. 2016, *A&A*, 594, A97 [2](#)
- Bersten, M., & Nomoto, K. 2014a, in *Binary Systems, their Evolution and Environments*, 36 [2](#)
- Brott, I., Evans, C. J., Hunter, I., et al. 2011, *A&A*, 530, A116 [2](#), [3](#), [4](#)
- Castor, J., McCray, R., & Weaver, R. 1975, *ApJ*, 200, L107 [2](#)
- Chen, X., Xu, Y., Shen, Z., & Li, J. 2006, *Science in China Series G: Physics, Mechanics and Astronomy*, 49, 1862 [7](#)
- Chiaki, G., Marassi, S., Nozawa, T., et al. 2015, *MNRAS*, 446, 2659 [3](#)
- Chieffi, A., & Limongi, M. 2004, *VizieR Online Data Catalog*, *J/ApJ/608/405* [2](#)
- Chieffi, A., & Limongi, M. 2013, *ApJ*, 764, 21 [5](#)
- Cui, Z., Wang, Z., Zhu, C., et al. 2018, *PASP*, 130, 084202 [2](#), [3](#)
- Curtis, S., Ebinger, K., Fröhlich, C., et al. 2019, *ApJ*, 870, 2 [3](#)
- de Mink, S. E., Langer, N., Izzard, R. G., Sana, H., & de Koter, A. 2013, *ApJ*, 764, 166 [2](#), [3](#)
- Du, F. 2020, arXiv e-prints, arXiv:2007.11294 [1](#)
- Dufton, P. L., Langer, N., Dunstall, P. R., et al. 2013, *A&A*, 550, A109 [2](#)
- Dunne, L., Eales, S., Ivison, R., Morgan, H., & Edmunds, M. 2003, *Nature*, 424, 285 [1](#)
- Duolikun, A., Zhu, C., Wang, Z., et al. 2019, *PASP*, 131, 124202 [1](#)
- Ekström, S., Meynet, G., Chiappini, C., Hirschi, R., & Maeder, A. 2008, *A&A*, 489, 685 [7](#)
- Eldridge, J. J., & Maund, J. R. 2016, *MNRAS*, 461, L117 [2](#)
- Fremming, C., Sollerman, J., Taddia, F., et al. 2014, *A&A*, 565, A114 [2](#)
- Glebbeek, E., Gaburov, E., de Mink, S. E., Pols, O. R., & Portegies Zwart, S. F. 2009, *A&A*, 497, 255 [2](#)
- Groenewegen, M., & de Jong, T. 1993, in *European Southern Observatory Conference and Workshop Proceedings*, Vol. 46, 101 [1](#)
- Groh, J. H., Meynet, G., & Ekström, S. 2014, *A&A*, 564, A30 [5](#)
- Guo, Y., Liu, D., Wu, C., & Wang, B. 2020, arXiv e-prints, arXiv:2008.00866 [1](#)
- Hamuy, M. 2003, *IAU Circ.*, 8146, 3 [8](#)
- Heger, A. 1998, *The presupernova evolution of rotating massive stars*, Garching, Germany: Max-Planck-Institut für Astrophysik, QB1000. H433 [2](#)

- Heger, A., & Langer, N. 2000, *ApJ*, 544, 1016 [2](#), [3](#)
- Heger, A., & Woosley, S. E. 2010, *ApJ*, 724, 341 [2](#)
- Higgins, E. R., & Vink, J. S. 2019, *A&A*, 622, A50 [2](#)
- Hirschi, R., Arnett, D., Cristini, A., et al. 2017, in *IAU Symposium*, Vol. 331, *Supernova 1987A:30 years later - Cosmic Rays and Nuclei from Supernovae and their Aftermaths*, ed. A. Marcowith, M. Renaud, G. Dubner, A. Ray, & A. Bykov, 1 [3](#)
- Hirschi, R., Meynet, G., & Maeder, A. 2005, *Nucl. Phys. A*, 758, 234 [5](#)
- Hirschi, R., Meynet, G., & Maeder, A. 2005b, *A&A*, 433, 1013 [5](#)
- Hix, W. R. 2001, *Nuclear Reaction Rate Uncertainties and Their Effects on Nova Nucleosynthesis Modeling*, arXiv: 08133, Tech. rep. [1](#)
- Hurley, J. R., Pols, O. R., & Tout, C. A. 2000, *MNRAS*, 315, 543 [2](#), [3](#)
- José, J., Hernanz, M., & Iliadis, C. 2006, *Nucl. Phys. A*, 777, 550 [1](#)
- Kippenhahn, R., Ruschenplatt, G., & Thomas, H. C. 1980, *A&A*, 91, 181 [3](#)
- Köhler, K., Langer, N., de Koter, A., et al. 2015, *A&A*, 573, A71 [2](#)
- Langer, N., Heger, A., & García-Segura, G. 1998, *Reviews in Modern Astronomy*, 11, 57 [2](#), [3](#)
- Li, F., Zhu, C., Lü, G., & Wang, Z. 2016, *PASJ*, 68, 39 [1](#)
- Limongi, M., & Chieffi, A. 2018, *ApJS*, 237, 13 [6](#)
- Lü, G., Zhu, C., & Podsiadlowski, P. 2013, *ApJ*, 768, 193 [1](#)
- Ma, Y.-C., Liu, H.-L., Zhu, C.-H., et al. 2020, *RAA*, 20, 049 [2](#)
- Maeder, A. 1975, *A&A*, 43, 61 [2](#)
- Maeder, A., & Meynet, G. 2001, *A&A*, 373, 555 [5](#)
- Maeder, A., & Meynet, G. 2012, *Reviews of Modern Physics*, 84, 25 [2](#)
- Mandel, I., & De Mink, S. 2016, in *41st COSPAR Scientific Assembly*, Vol. 41, E1.16 [2](#)
- Marassi, S., Schneider, R., Limongi, M., et al. 2019, *MNRAS*, 484, 2587 [2](#), [7](#), [8](#)
- Marchant, P., Langer, N., Podsiadlowski, P., Tauris, T. M., & Moriya, T. J. 2016, *A&A*, 588, A50 [2](#)
- Marigo, P. 2007, in *Astronomical Society of the Pacific Conference Series*, Vol. 378, *Why Galaxies Care About AGB Stars: Their Importance as Actors and Probes*, ed. F. Kerschbaum, C. Charbonnel, & R. F. Wing, 392 [1](#)
- Meyer, D. M. A., Petrov, M., & Pohl, M. 2020, *MNRAS*, 493, 3548 [5](#)
- Meynet, G. 2000, in *IAU Joint Discussion*, Vol. 24, 11 [2](#)
- Meynet, G. 2012, in *Chemical Evolution of the Milky Way*, 20 [3](#)
- Meynet, G., & Maeder, A. 2006, *Single Massive Stars at the Critical Rotational Velocity*, *Astronomical Society of the Pacific Conference Series*, 355, 27 [2](#)
- Mokiem, M. R., de Koter, A., Vink, J. S., et al. 2007, *A&A*, 473, 603 [2](#)
- Moravveji, E. 2016, *MNRAS*, 455, L67 [2](#)
- Nomoto, K., Kobayashi, C., & Tominaga, N. 2013, *Annual Review of Astronomy and Astrophysics*, 51, 457 [2](#), [8](#)
- Nomoto, K., Tominaga, N., Tanaka, M., Maeda, K., & Umeda, H. 2007, in *American Institute of Physics Conference Series*, Vol. 937, *Supernova 1987A: 20 Years After: Supernovae and Gamma-Ray Bursters*, ed. S. Immler, K. Weiler, & R. McCray, 412 [3](#)
- Nomoto, K., Tominaga, N., Umeda, H., Kobayashi, C., & Maeda, K. 2006, *Nucl. Phys. A*, 777, 424 [2](#)
- Nugis, T., & Lamers, H. J. G. L. M. 2000, *A&A*, 360, 227 [4](#)
- Paxton, B., Bildsten, L., Dotter, A., et al. 2011, *ApJS*, 192, 3 [2](#)
- Paxton, B., Cantiello, M., Arras, P., et al. 2013, *ApJS*, 208, 4 [2](#), [3](#)
- Paxton, B., Marchant, P., Schwab, J., et al. 2015, *ApJS*, 220, 15 [2](#)
- Pinsonneault, M. H., Kawaler, S. D., Sofia, S., & Demarque, P. 1989, *ApJ*, 338, 424 [2](#), [3](#)
- Prantzos, N., Abia, C., Limongi, M., Chieffi, A., & Cristallo, S. 2018, *MNRAS*, 476, 3432 [2](#)
- Puls, J., Vink, J. S., & Najarro, F. 2008, *A&A Rev.*, 16, 209 [2](#)
- Rukeya, R., Lü, G., Wang, Z., & Zhu, C. 2017, *PASP*, 129, 074201 [1](#)
- Shi, Y., Xue, X., Zhu, C., et al. 2020, *RAA*, v.20, 37 [1](#), [2](#)
- Smith, N. 2014, *Constraining the Mass in Cool Dust Shells Around Massive Stars* [2](#)
- Song, H. F., Meynet, G., Maeder, A., Ekström, S., & Eggenberger, P. 2016, *A&A*, 585, A120 [2](#)

- Thielemann, F. K., Dillmann, I., Farouqi, K., et al. 2010, in *Journal of Physics Conference Series*, Vol. 202, 012006 [3](#)
- Tominaga. 2008, *The Astrophysical Journal*, 690, 526 [6](#)
- van Marle, A. J., Langer, N., Achterberg, A., & García-Segura, G. 2007, 30, 1 [6](#)
- Viallet, M., Meakin, C., Prat, V., & Arnett, D. 2015, *A&A*, 580, A61 [2](#)
- Vink, J. S. 2000, *Radiation-driven Wind Models of Massive Stars*, PhD thesis, Universiteit Utrecht [2](#)
- Vink, J. S., de Koter, A., & Lamers, H. J. G. L. M. 2001, *A&A*, 369, 574 [2, 3, 4](#)
- Wang, T., Li, L., Zhu, C., et al. 2018, *ApJ*, 863, 17 [2, 3](#)
- Woosley, S. E., & Weaver, T. A. 1995, *ApJS*, 101, 181 [2](#)
- Yoon, S. C., Dierks, A., & Langer, N. 2012, *A&A*, 542, A113 [3](#)
- Yoon, S. C., & Langer, N. 2006, in *Astronomical Society of the Pacific Conference Series*, Vol. 353, *Stellar Evolution at Low Metallicity: Mass Loss, Explosions, Cosmology*, ed. H. J. G. L. M. Lamers, N. Langer, T. Nugis, & K. Annuk, 63 [3](#)
- Zhu, C., Liu, H., Lü, G., Wang, Z., & Li, L. 2019, *MNRAS*, 488, 525 [1](#)
- Zhu, C., Lü, G., & Wang, Z. 2017, *ApJ*, 835, 249 [3](#)
- Zhu, C., Lü, G., Wang, Z., & Liu, J. 2013, *PASP*, 125, 25 [1](#)